

Insights into Mechanistic Photodissociation of Acetyl Chloride by *ab Initio* Calculations and Molecular Dynamics Simulations[†]

Shi-Lu Chen and Wei-Hai Fang*

College of Chemistry, Beijing Normal University, Beijing 100875, People's Republic of China

Received: May 19, 2007; In Final Form: June 24, 2007

The potential energy surfaces of dissociation and elimination reactions for CH₃COCl in the ground (S₀) and first excited singlet (S₁) states have been mapped with the different *ab initio* calculations. Mechanistic photodissociation of CH₃COCl has been characterized through the intrinsic reaction coordinate and *ab initio* molecular dynamics calculations. The α-C–C bond cleavage along the S₁ pathway leads to the fragments of COCl(²A'') and CH₃(²A') in an excited electronic state and a high barrier exists on the pathway. This channel is inaccessible in energy upon photoexcitation of the CH₃COCl molecules at 236 nm. The S₁ α-C–Cl bond cleavage yields the Cl(²P) and CH₃CO(³X²A') fragments in the ground state and there is very small or no barrier on the pathway. The S₁ α-C–Cl bond cleavage proceeds in a time scale of picosecond in the gas phase, followed by CH₃CO decomposition to CH₃ and CO. The barrier to the C–Cl bond cleavage on the S₁ surface is significantly increased by effects of the argon matrix. The S₁ α-C–Cl bond cleavage in the argon matrix becomes inaccessible in energy upon photoexcitation of CH₃COCl at 266 nm. In this case, the excited CH₃COCl(S₁) molecules cannot undergo the C–Cl bond cleavage in a short period. The internal conversion from S₁ to S₀ becomes the dominant process for the CH₃COCl(S₁) molecules in the condensed phase. As a result, the direct HCl elimination in the ground state becomes the exclusive channel upon 266 nm photodissociation of CH₃COCl in the argon matrix at 11 K.

Introduction

Acetyl chloride (CH₃COCl) is an important organic compound and particular attention has been recently devoted to its photodissociation in both the gas and solid phases.^{1–9} The photodissociation of CH₃COCl is interesting from both an environmental and fundamental chemistry perspective.^{1,10,11} The discharge of chlorine-containing compounds into the environment has raised concern regarding their potential impact on stratospheric ozone abundances and groundwater supplies.^{11,12} In addition, the acetyl radical (CH₃CO) is one of the important intermediates in combustion processes and atmospheric reactions, and studies on electronic structure and dissociation dynamics of this radical are very helpful for atmospheric chemistry.^{13,14} The C–Cl bond cleavage of CH₃COCl is one of main pathways for generating CH₃CO radical.

Photofragment ion imaging technique was used to study the photodissociation of gaseous CH₃COCl at 236 nm.^{4,5} The decomposition products formed following irradiation are atomic chlorine (Cl), acetyl radical, methyl radical (CH₃), and carbon monoxide (CO); no other photoproducts are observed in the gas phase. Crossed laser-molecular beam experiments^{6,7} showed one primary dissociation channel of gaseous CH₃COCl, the C–Cl bond fission:



The formed CH₃CO radical undergoes secondary dissociation to produce CO and CH₃ with a significant amount of energy partitioned into translational motion:^{4,5}



In order to explore dissociation behavior of acetyl radical, photolysis of gaseous CH₃COCH₃ at 193 and 248 nm has been studied by molecular beam photofragment translational spectroscopy.¹⁵ Energy barrier of the radical dissociation (eq 1.1) was experimentally estimated to be 17.8 ± 3.0 kcal/mol. The C–C and C–Cl bonds have similar strength and the α-C–C bond cleavage might take place after photoexcitation of gaseous CH₃COCl at 236 nm or shorter wavelengths:



The COCl radical is very unstable and can decompose into CO and Cl:



But the photoproducts of CH₃ and COCl (CO and Cl) were not observed in the photolysis of gaseous CH₃COCl. Photofragment ion imaging with femtosecond real-time clocking has been applied the C–Cl bond cleavage from the ¹nπ* state of gaseous CH₃COCl.¹⁶ It was found that the cleavage occurs within the time comparable with laser pulse duration of 200 fs.

To understand the mechanism of the CH₃COCl photodecomposition in the condensed phase, Rowland and Hess^{8,9} have used polarized Fourier transform infrared (FTIR) absorption spectroscopy to probe the photodecomposition products of acetyl chloride in an Ar matrix at 11 K following irradiation at 266 nm. The observed products are ketene (CH₂=C=O) and hydrochloric acid (HCl):



[†] Part of the "Sheng Hsien Lin Festschrift".

* Corresponding author. Tel.: +86-10-58805382. Fax: +86-10-5880-2075. E-mail: Fangwh@bnu.edu.cn.

No other products were detected even after prolonged irradiation of CH_3COCl in the condensed phase. Acetyl chloride in an argon matrix was found to decompose on irradiation into ketene and hydrogen chloride, which formed the ketene $\cdots\text{HCl}$ complex.¹⁷ The fundamental vibrational frequency of HCl in the complex was observed at 2679 cm^{-1} , 191 cm^{-1} below the frequency of the corresponding HCl monomer in solid argon. It is evident that the observed photoproducts are dependent on the initial phases of the reactant.

Photolysis of matrix-isolated CF_3COCl has been investigated with IR spectroscopy and it was found that CF_3COCl is decomposed in an argon matrix to produce CF_3Cl and CO. A radical mechanism was suggested for formation of CF_3Cl and CO.¹⁸ Matrix isolation study on the photolysis of CCl_3COCl has been performed, and CCl_4 and CO were found to be dominant products in the Ar matrix.¹⁹ But the CCl_3 and COCl radicals were observed as intermediates, indicating that the C–C bond cleavage occurs in the matrix. The marked difference exists in mechanistic photochemistry of matrix-isolated CH_3COCl and CCl_3COCl , which was attributed to the triplet surface reaction of CCl_3COCl .

As a complementary of experimental works, structural parameters, fundamental vibrational frequencies, and relative energies of CH_3COCl and CH_3CO in the ground state were determined from several theoretical calculations.^{20–23} At the UHF level of theory, optimal geometries for CH_3CO have been reported by Francisco and Abersold²⁰ with the 6-31G(d) basis set and by Nimlos et al.²¹ with the larger 6-311++G(d,p) basis set. The differences in the geometry with these two basis sets are very small. Sumathi and Chandra optimized the geometries of CH_3COCl and CH_3CO at the MP2 level of theory with the 6-31G(d) and 6-31G(d,p) basis sets.^{22a} In addition, energy barrier for CH_3CO dissociation is predicted to be 19.1 kcal/mol at the MP2/cc-pVTZ level by Deshmukh et al.⁵ The structures of CH_3COCl in the S_1 and T_1 electronic states were calculated by the MP2 and CASSCF methods.²⁴ It was found that electronic excitation causes considerable conformational changes involving rotation of the CH_3 top and a substantial deviation of the CCOCl fragment from planarity. In addition, two-dimensional potential energy surface was calculated for torsional-inversion in the S_1 and T_1 states. As far as we know, there is no ab initio study on the photolysis of CH_3COCl in the gas and condensed phases.

The photoreactivity of acetyl chloride is highly sensitive to the initial phase of the reactant and the photoproducts in the gas phase are completely different from those in the condensed phase. Although there are several experimental studies regarding photodissociation of CH_3COCl in the gas and condensed phases, the inferences about the mechanisms are rather speculative and not well substantiated in the previous studies. The most pressing issue is mechanistic photodissociation of CH_3COCl in the condensed phase. The C–Cl bond cleavage in the gas-phase takes place in a time scale of ps. If the S_1 – S_0 internal conversion in the Franck–Condon region and the subsequent elimination of HCl in the condensed phase are more rapid than the C–Cl bond cleavage in the gas phase, the time scale for these processes in the condensed phase is on the order of fs. Obviously, this is an unreasonable conclusion. The C–C and C–Cl bonds have similar strength in CH_3COCl . It can be expected that the α -C–C and α -C–Cl bond cleavages could be competitive with each other upon photoexcitation of CH_3COCl at 236 nm. However, only the fragments from the C–Cl bond fission were observed by photolysis of CH_3COCl in the gas phase. The underlying reason is not completely clear.

To provide new insights into the mechanistic photochemistry of acetyl chlorides and related compounds, we took CH_3COCl as a representative in the present work, and have carried out density functional theory (DFT) and complete active space self-consistent field (CASSCF) studies on potential energy surfaces of the CH_3COCl dissociation in the S_0 and S_1 states. Ab initio molecular dynamics calculations were conducted to determine the initial relaxation process from the S_1 Franck–Condon geometry and the HCl elimination dynamics. The S_1 C–Cl bond cleavage is predicted to occur in about 200 fs and is the dominant primary process upon photodissociation of CH_3COCl in the gas phase. The polarized continuum model (PCM) was used to simulate effect of argon at 11 K on the C–Cl bond cleavage along the S_1 pathway. The barrier to the C–Cl bond cleavage on the S_1 surface is significantly increased by effects of the matrix and the internal conversion to the ground state prevails. The direct HCl elimination becomes the dominant channel upon photodissociation of CH_3COCl in the argon matrix at 11 K.

Computational Methods

Stationary structures on the S_0 potential energy surface (PES) have been optimized with the B3LYP method, which is composed of Becke's three-parameter hybrid exchange functional (B3)²⁵ and the correlation functional of Lee, Yang, and Parr (LYP).²⁶ The harmonic vibrational frequencies were examined to confirm the optimized structure to be a true minimum or first-order saddle point on the S_0 PES. The intrinsic reaction coordinate (IRC) calculations have been carried out at the B3LYP level with the saddle-point structures as the starting points, in order to confirm the optimized saddle point to be on the correct reaction pathway. The complete-active-space self-consistent field (CASSCF) wave function has sufficient flexibility to model the changes in electronic structure upon electronic excitation,^{27,28} which is employed to optimize stationary structures on the S_1 potential energy surface of the C–Cl and C–C bond fissions. In the CASSCF calculations, the active space is composed of ten electrons distributed in eight orbitals, referred to as CAS(10,8) hereafter. The CAS(10,8) calculation is related to finite inclusion of electron correlation effect. To make compensation for this, the single-point energy is calculated with the multireference configuration interaction (MR-CI) method on the CAS(10,8) wave functions. The cc-pVDZ and cc-pVTZ basis sets²⁹ are used in the present study. The CASSCF and DFT calculations were performed using the Gaussian 98 and 03 packages of programs,³⁰ while the MOLPRO program package³¹ was used to perform the MR-CI calculations.

The polarized continuum model (PCM)³² was used to simulate effect of argon at 11 K on the C–Cl bond cleavage along the S_1 pathway. The dielectric constant of 2.38 and temperature of 11 K were selected to simulate effect of the matrix with the PCM model. Ab initio classical trajectory calculations^{33,34} were performed using a Born–Oppenheimer molecular dynamics model.^{35,36} The trajectories start at the transition state of the HCl elimination, and were stopped when the centers of mass of the products were 12 bohr apart. Fifty trajectories were integrated at the B3LYP/cc-pVDZ level for the HCl elimination of CH_3COCl in the ground state. The initial conditions for the trajectory calculations were chosen to simulate photolysis of CH_3COCl at 236 nm with the initial kinetic energy that corresponds to the energy difference between 236 nm photon and the transition state of the HCl elimination. The total angular momentum was set to zero. The Hessian was updated for 5 steps

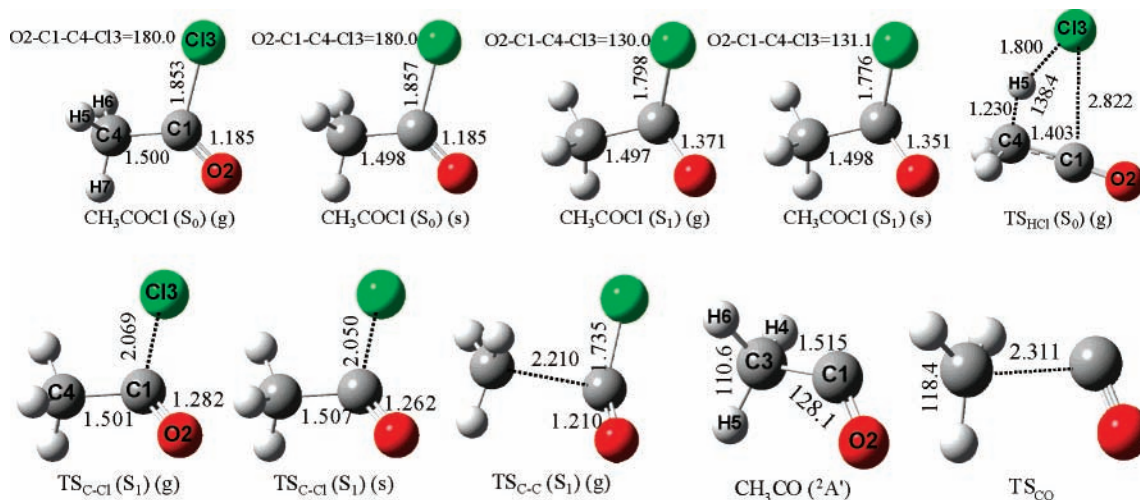


Figure 1. The stationary structures along with the key B3LYP/cc-pVDZ bond parameters for $\text{TS}_{\text{HCl}}(S_0)$, $\text{CH}_3\text{CO}(^2A')$, and TS_{CO} , and the CAS(10,8)/cc-pVDZ bond parameters for other geometries (bond lengths in Å, and bond angles and dihedral angles in degree). g and s denote the bond parameters optimized at the gas phase and argon matrix with the PCM model, respectively.

before being recalculated analytically. A step size of 0.25 $\text{amu}^{1/2}\text{bohr}$ was used for all of the trajectory calculations.

Results and Discussion

Equilibrium Geometries. Equilibrium geometry and electronic structure are basic, but very important, properties of a molecule. Experimentally, microwave spectroscopy³⁷ and gas-phase electron diffraction experiment³⁸ showed that CH_3COCl in the ground state exists as a single conformer, which is labeled by $\text{CH}_3\text{COCl}(S_0)$ in Figure 1. The CH_3COCl molecule in ground state has C_s symmetry with all of the heavy atoms and one of the methyl hydrogen atoms in the plane of symmetry. The experimentally inferred $\text{CH}_3\text{COCl}(S_0)$ structure^{5,22,39} are well reproduced by the previous MP2 calculation with the 6-311G(d,p) basis set and the present B3LYP and CAS(10,8) calculations with cc-pVDZ and cc-pVTZ basis sets (Supporting information).

The S_1 equilibrium geometry of CH_3COCl is optimized with the CAS(10,8)/cc-pVDZ approach. The resulting structure is shown in Figure 1, along with the key CAS(10,8)/cc-pVDZ bond parameters. In comparison with the equilibrium geometry in the ground state, the C1-O2 bond length is elongated by 0.186 Å in the S_1 structure. The O2-C1-C4-Cl3 dihedral angle is decreased from 180.0° in the S_0 structure to 130.0° in the S_1 structure. Natural orbital analysis clearly shows that the S_1 state originates from the $n \rightarrow \pi^*$ excitation. One electron excitation from n to π^* orbital leads to a partial breaking of the C=O π bond. As a result of this, the C-O bond is significantly elongated in S_1 with respect to that in S_0 . From the viewpoint of valence bond theory, the $n \rightarrow \pi^*$ excitation makes the carbonyl C atom rehybridize from sp^2 in the ground state to sp^3 in the S_1 state, resulting in the S_1 pyramidal structure at the carbonyl carbon atom. The similar results were obtained from the CAS(10,8)/cc-pVTZ calculations. It is obvious that the present CASSCF calculations provide a good description on the structures of CH_3COCl in the S_0 and S_1 states. In fact, the S_1 state has common pyramidal equilibrium geometry for a wide variety of aliphatic carbonyl molecules.⁴⁰⁻⁴³

α -Elimination of HCl. The dissociation of CH_3COCl into $\text{CH}_2\text{CO} + \text{HCl}$ is generally assigned as an α -elimination process. A transition state was optimized at the B3LYP/cc-pVDZ and B3LYP/cc-pVTZ levels and confirmed to be the first-order saddle point on the S_0 pathway, which is denoted by $\text{TS}_{\text{HCl}}(S_0)$. Its structure is shown in Figure 1 along with B3LYP/

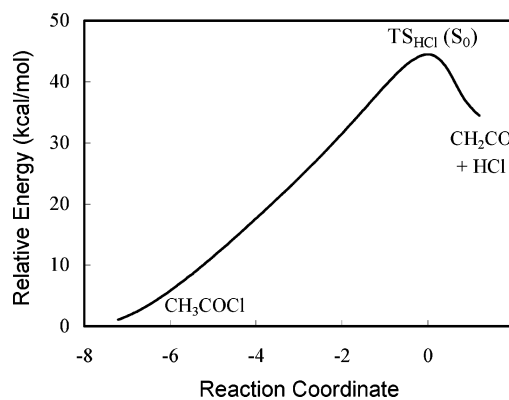


Figure 2. Schematic potential energy surfaces of the HCl elimination reactions.

cc-pVDZ bond parameters. The C1-Cl3 and H5-Cl3 distances are respectively 2.822 and 1.800 Å in the $\text{TS}_{\text{HCl}}(S_0)$ structure. The large C1-Cl3 separation gives us a hint that $\text{TS}_{\text{HCl}}(S_0)$ could be a transition state for hydrogen abstraction of the acetyl radical by the free chlorine atom. In order to confirm $\text{TS}_{\text{HCl}}(S_0)$ to be the transition state of the direct HCl elimination, the IRC calculations were carried out at the B3LYP/cc-pVDZ level with the $\text{TS}_{\text{HCl}}(S_0)$ structure as the starting point. $\text{TS}_{\text{HCl}}(S_0)$ was confirmed to connect the CH_3COCl on the reactant side and $\text{CH}_2\text{CO} + \text{HCl}$ on the product side. Energies from the IRC calculations are plotted in Figure 2 as a function of reaction coordinate. The direct α -elimination of HCl has a barrier of 44.5 kcal/mol at the B3LYP/cc-pVDZ level and 44.2 kcal/mol at the B3LYP/cc-pVTZ level. The barrier becomes 40.7 and 40.6 kcal/mol with the zero-point energy correction included at the B3LYP/cc-pVDZ and B3LYP/cc-pVTZ levels, respectively.

The IRC calculations ignore the effects of vibrational and kinetic energies on the reaction processes. It has been shown that reactions do not necessarily follow the IRC pathways when kinetic energy is accounted for.^{44,45} In view of this, the dissociation of CH_3COCl to $\text{CH}_2\text{CO} + \text{HCl}$ has been studied by direct classical trajectory calculations using the B3LYP/cc-pVDZ method. The initial conditions for the trajectory calculations were chosen to simulate photolysis of CH_3COCl at 236 nm with the initial kinetic energy of 76.6 kcal/mol, which corresponds to the energy difference between 236 nm photon (121.1 kcal/mol) and the $\text{TS}_{\text{HCl}}(S_0)$ energy (44.5 kcal/mol). The

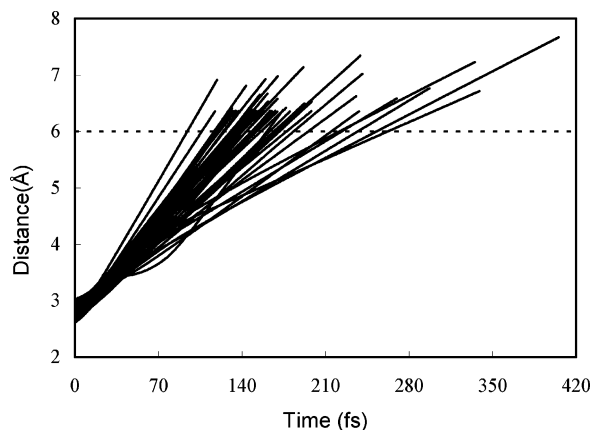


Figure 3. The distances between the centers of mass for HCl and CH₂CO are plotted as functions of time for the fifty trajectories.

distances between the centers of mass are plotted in Figure 3 as a function of time for all fifty trajectories. The two fragments of HCl and CH₂CO are completely separated (larger than 12 bohr) after 250 fs propagations of the trajectories. This gives further evidence that the α -elimination of HCl from CH₃COCl is a direct elimination process with CH₂CO as coproduct.

All attempts to optimize a transition state for the direct α -elimination of HCl on the S₁ state were unsuccessful. The direct α -elimination of HCl involves cleavages of the C–Cl and C–H bonds, formation of the H–Cl bond, and a large deformation of the molecular structure, simultaneously. It is reasonable to expect that on the S₁ state the direct α -elimination should not compete with the C–Cl bond fission and other photophysical processes. Ketene (CH₂=C=O) and HCl were observed as exclusive products upon photodissociation of CH₃COCl in the argon matrix at 11 K.^{8,9} The α -elimination of HCl was proposed to proceed directly along the S₀ pathway as a result of internal conversion from an excited singlet state. Both the present theoretical calculations and the previous experimental observations agree in predicting that the direct α -elimination of HCl occurs on the S₀ surface.

α -C–Cl and C–C Bond Cleavages. Photoexcitation of a carbonyl compound from the ground state (S₀) to its first excited state (S₁) leads primarily to the cleavage of a bond α to the carbonyl group, which is referred to as Norrish type I reaction. There are comparable pre-exponential factors for different bond fissions, and the relative strengths of the alpha bonds closely approximate the relative barrier heights. It is generally thought that the weaker of the two α bonds cleaves most readily upon low-energy photon excitation. However, the experimental investigations^{1–7} on photodissociation of CH₃COCl have demonstrated that the α -C–Cl bond breaks in high yield and cleavage of the α -C–C bond occurs with little probability, although the two α bonds have similar strength with the dissociation energy of about 80 kcal/mol.⁴⁶ Here, the potential energy surfaces of the α -C–Cl and α -C–C bond cleavages were determined by the combined MR–CI and CASSCF calculations.

Both COCl and CH₃ radicals have ²A' symmetry in the ground state. When the two ground-state radicals approach each other in C₁ symmetry, they can correlate with CH₃COCl in the S₀ state. Therefore, the CH₃COCl in the S₁ state only can correlate with the COCl(²A'') and CH₃(²A') fragments in an excited electronic state. Unlike the α C–C bond cleavage, fission of the α -C–Cl bond produces the Cl(²P) atom, which is 3-fold degenerate. When the Cl(²P) atom and the CH₃CO(\tilde{X}^2A') radical approach each other in C₁ symmetry, they can correlate adiabatically with the S₀, S₁, and S₂ states of CH₃COCl.

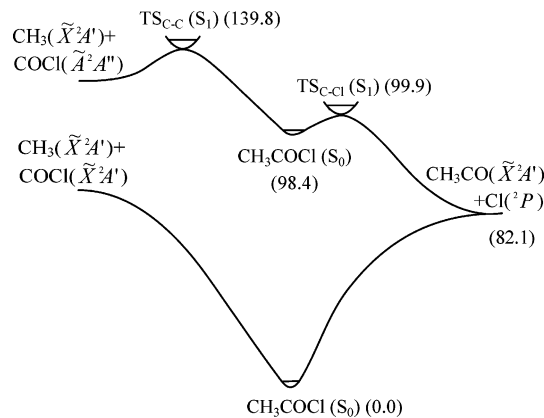


Figure 4. Schematic potential energy profiles for the C–C and C–Cl bond cleavages of CH₃COCl in the S₀ and S₁ states, along with the MR–CI relative energy (kcal/mol).

The qualitative state correlation analysis is consistent with the calculated potential energy surfaces of α -C–Cl and C–C bond cleavages, which will be discussed below.

CH₃COCl may dissociate into CH₃CO + Cl and CH₃ + COCl along the ground-state pathways. We have made efforts to optimize a transition state for the α -C–Cl or α -C–C bond cleavage in the ground state, but optimizations always lead to the dissociation limit of CH₃CO + Cl or CH₃ + COCl. It is evident that no potential barrier above the endothermicity exists on the S₀ pathway to CH₃CO + Cl or CH₃ + COCl.

The adiabatic excitation energy (0–0 energy gap) from S₀ to S₁ was first calculated with the CAS(10,8)/cc-pVDZ approach, which gives the value of 103.2 kcal/mol for the S₀ → S₁ transition of CH₃COCl. On the basis of the CAS(10,8)/cc-pVDZ optimized structures for the S₀ and S₁ states, the 0–0 energy gap was predicted to be 98.4 kcal/mol by the MR–CI single-point energy calculations. As far as we know, the band origin for the S₀ → S₁ transition of CH₃COCl was not reported in the literature up to date. Two transition states, referred to as TS_{C–C}(S₁) and TS_{C–Cl}(S₁) hereafter, were found on the S₁ surface and confirmed to be the first-order saddle points by frequency calculations. The imaginary vibrational modes show that TS_{C–C}(S₁) and TS_{C–Cl}(S₁) are the transition states on the S₁ pathways to CH₃(\tilde{X}^2A') + COCl(\tilde{A}^2A'') and CH₃CO(\tilde{X}^2A') + Cl(²P), respectively. At the CAS(10,8)/cc-pVDZ level, the C–C distance is 2.210 Å in TS_{C–C}(S₁) and the C–Cl distance is 2.069 Å in TS_{C–Cl}(S₁), which are 0.713 and 0.271 Å longer than the corresponding values in the S₁ minimum. With respect to the vibrational zero-level of the S₁ state, the barrier heights for the C–C and C–Cl bond fissions on the S₁ surface are 45.8 and 4.0 kcal/mol at the CAS(10,8)/cc-pVDZ level, respectively. They become 41.4 and 1.5 kcal/mol by the MR–CI single-point energy calculations. The potential energy surfaces for the C–C and C–Cl bond cleavages are shown in Figure 4, along with the MR–CI relative energies. It is obvious that the S₁ barrier to the α -C–Cl bond cleavage is much lower than that for the α -C–C bond fission along the S₁ pathway. As discussed before, the S₁ C–C bond fission leads to the CH₃(\tilde{X}^2A') + COCl(\tilde{A}^2A'') fragments in the excited-state with high endothermicity, while the S₁ C–Cl bond cleavage produces the CH₃CO(\tilde{X}^2A') + Cl(²P) fragments in the ground state and is exothermic by about 20 kcal/mol. These are main reasons why the S₁ C–C bond fission has a barrier that is much higher than that for the S₁ C–Cl bond cleavage, which provides a reasonable explanation why the C–Cl bond cleavage was experimentally observed to be dominant channel upon n→ π^* excitation of CH₃COCl in the gas phase.

The formed CH_3CO radical can undergo secondary dissociation to produce CO and CH_3 in the ground state. In order to elucidate the mechanism of CH_3CO dissociation, the geometries of the $^2\text{A}'$ ground state of CH_3CO and transition state for the CH_3CO dissociation were optimized at the B3LYP/cc-pVDZ and B3LYP/cc-pVTZ levels. The optimized structure of CH_3CO in the ground state, labeled as $\text{CH}_3\text{CO}(^2\text{A}')$, is shown in Figure 1 along with the B3LYP/cc-pVDZ bond parameters.

The structure of transition state for the CH_3CO dissociation, denoted by TS_{CO} , is given in Figure 1 along with the key B3LYP/cc-pVDZ parameters. It can be seen from the TS_{CO} structure that the $\text{C1}-\text{C3}$ bond is elongated by 0.796 \AA with respect to $\text{CH}_3\text{CO}(^2\text{A}')$. As opposed to $\text{CH}_3\text{CO}(^2\text{A}')$, the $\text{H}-\text{C3}-\text{H}$ angle increases from 110.6° to 118.4° , which implies the rehybridization of C3 atom from sp^3 to sp^2 . The CH_3CO dissociation has a barrier of 20.4 kcal/mol at the B3LYP/cc-pVDZ level and 19.6 kcal/mol at the B3LYP/cc-pVTZ level. The barrier becomes 17.0 and 16.3 kcal/mol with the zero-point energy correction included at the B3LYP/cc-pVDZ and B3LYP/cc-pVTZ levels, respectively. These results satisfactorily agree with that obtained from molecular beam photofragment translational spectroscopy ($17.8 \pm 3.0 \text{ kcal/mol}$),²⁰ after photoexcitation of CH_3COCl at 236 nm , the $\text{CH}_3\text{COCl}(\text{S}_1)$ molecule has sufficient internal energies to overcome the barrier to $\alpha\text{-C}-\text{Cl}$ bond cleavage and rapidly decompose into CH_3CO and Cl in the gas phase. In this case, the formed CH_3CO radical can further dissociate into CH_3 and CO .

Here we performed ab initio molecular dynamic calculation to provide further evidence for the rapid S_1 $\text{C}-\text{Cl}$ bond cleavage. The initial conditions for trajectory calculations have been chosen to simulate the experimental photodissociation of CH_3COCl at 236 nm . Trajectory starts from the S_1 Franck-Condon (FC) geometry with the initial kinetic energy of 5.0 kcal/mol , which is randomly distributed among the vibrational degrees of freedom. The potential energy and the key bond parameters as a function of time are plotted in Figure 5. The $\text{C}-\text{Cl}$ bond length is decreased to the S_1 equilibrium value at the initial stage and then the $\text{C}-\text{Cl}$ bond cleaves after 200 fs . The $\text{C}-\text{O}$ bond length is 1.185 \AA at the starting point of the trajectory, and increases very fast to a maximum value of 1.673 \AA . After 200 fs propagation, the $\text{C}-\text{O}$ bond length oscillates in the vicinity of 1.20 \AA . Similarly, the $\text{O2}-\text{C1}-\text{C4}-\text{Cl3}$ dihedral angle is changed from 180.0° at the S_1 FC structure to about 130° in the vicinity of the S_1 minimum and to about 90° in the fragment region. The corresponding changes in energy can be seen from Figure 5. On average, the trajectory reaches the $\text{TS}_{\text{C}-\text{Cl}}(\text{S}_1)$ region after 70 fs propagation and mainly move about in the fragment region after 200 fs . Ab initio molecular dynamics calculations predict that the S_1 $\alpha\text{-C}-\text{Cl}$ bond cleavage occurs within 200 fs . Photofragment ion imaging with femtosecond real-time clocking has been applied the $\text{C}-\text{Cl}$ bond cleavage from the $^1\text{n}\pi^*$ state of gaseous CH_3COCl .¹⁶ It was found that the cleavage occurs within the time comparable with laser pulse duration of 200 fs .

The Argon Matrix Effect. The HCl elimination was detected to be an exclusive channel for the CH_3COCl photodecomposition in the Ar matrix at 11 K .^{8,9} The rapid cleavage of $\text{C}-\text{Cl}$ bond observed in the gas phase was not found in the condensed-phase reaction.⁸ The PCM model was used to simulate effect of argon at 11 K on the $\text{C}-\text{Cl}$ bond cleavage along the S_1 pathway. The S_1 equilibrium geometry and the $\text{TS}_{\text{C}-\text{Cl}}(\text{S}_1)$ structure in the Ar matrix at 11 K (Figure 1) were optimized at the CAS(10,8)/cc-pVDZ level, which predicts that the barrier to the S_1 $\text{C}-\text{Cl}$ bond fission is 15.3 kcal/mol in the argon matrix.

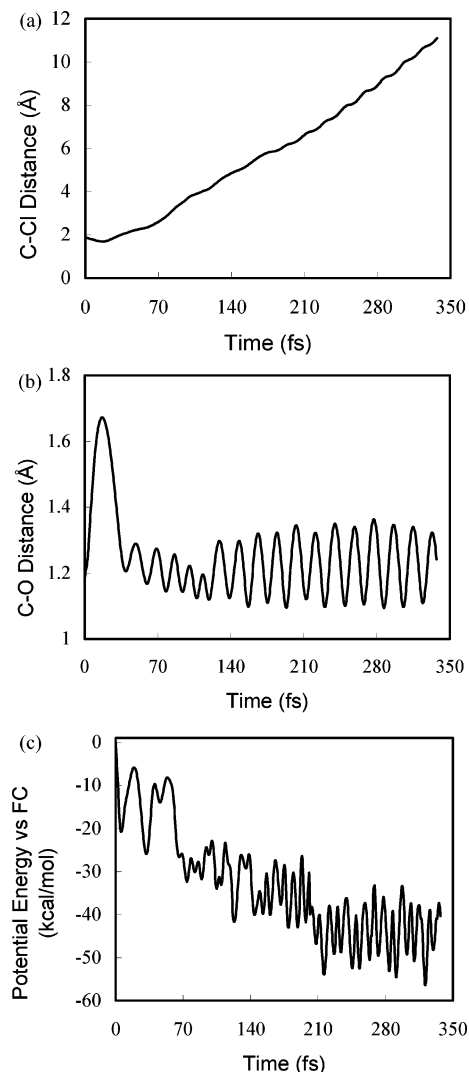


Figure 5. The $\text{C}-\text{Cl}$ distance (a), the $\text{C}-\text{O}$ distance (b), and the CASSCF energies (c) are plotted as functions of time for the trajectory starting from the S_1 Franck-Condon geometry.

As pointed out before, the $\text{C}-\text{Cl}$ bond fission along the S_1 pathway has a barrier of 4.0 kcal/mol at the CAS(10,8)/cc-pVDZ level for CH_3COCl in the gas phase. The matrix effects can be split into two contributions: geometry relaxation and intermolecular interaction between matrix and the investigated system. At the fixed structures of $\text{CH}_3\text{COCl}(\text{S}_1)$ and $\text{TS}_{\text{C}-\text{Cl}}(\text{S}_1)$ in the gas phase, the single-point energies were calculated with the PCM model at the CAS(10,8)/cc-pVDZ level. In comparison with the $\text{TS}_{\text{C}-\text{Cl}}(\text{S}_1)$ relative energy (4.0 kcal/mol) in the gas phase, the barrier to the S_1 $\text{C}-\text{Cl}$ bond fission was estimated to be increased by 5.4 kcal/mol due to the intermolecular interaction between the system and the matrix. It can be deduced that the geometry relaxation results in an increase of barrier height by 5.9 kcal/mol . The geometry relaxation and intermolecular interaction have similar contributions to the Ar matrix effect on the S_1 $\text{C}-\text{Cl}$ bond fission of CH_3COCl . As shown in Figure 1, the $\text{C}-\text{Cl}$ and $\text{C}-\text{O}$ distances are decreased by about 0.02 \AA from the gas phase to the argon matrix at 11 K .

Rowland and Hess^{8,9} have probed the photodecomposition products ($\text{HCl} + \text{CH}_2\text{C}=\text{C}=\text{O}$) of acetyl chloride in an Ar matrix at 11 K following irradiation at 266 nm . At this excitation wavelength, the S_1 $\alpha\text{-C}-\text{Cl}$ bond cleavage is energetically inaccessible on the basis of the CAS(10,8)/cc-pVDZ calculated relative energy for $\text{TS}_{\text{C}-\text{Cl}}(\text{S}_1)$ with the PCM model. It should

be pointed out that the relative energies of the S_1 stationary structures are overestimated by the CAS(10,8)/cc-pVDZ calculation. For instance, the geometry relaxation results in an increase of barrier height by 5.9 kcal/mol at the CAS(10,8)/cc-pVDZ level, but the barrier is predicted to be increased by 2.5 kcal/mol at the MR-Cl/cc-pVDZ level due to the geometry relaxation. Adiabatic RRKM theory of rate with tunneling effect^{47,48} is employed to calculate the rate constant of the α -C–Cl bond cleavage along the S_1 pathway. Since rotational degrees of freedom have less effect on the RRKM rate constant, only vibrational degrees of freedom are considered with a harmonic approximation. On the basis of the CAS(10,8) frequencies and the MR-Cl energies for $\text{CH}_3\text{COCl}(S_1)$ and $\text{TS}_{\text{C-Cl}}(S_1)$ in the argon matrix, the RRKM rate constant is predicted to $8.5 \times 10^7 \text{ s}^{-1}$ for the S_1 α -C–Cl bond cleavage of CH_3COCl in the argon matrix with a total angular momentum of $J = 0$ and a total energy of $E = 9.9$ kcal/mol, which corresponds to excitation energy at 266 nm with respect to the S_1 minimum.

In the Ar matrix, the excited $\text{CH}_3\text{COCl}(S_1)$ molecules can undergo the C–Cl bond cleavage in a period of 10^{-7} s. In this case, the interaction with the argon matrix probably results in deactivation of the excited $\text{CH}_3\text{COCl}(S_1)$ molecules through energy transfer to the matrix. As a result, the internal conversion from S_1 to S_0 becomes the dominant process for the $\text{CH}_3\text{COCl}(S_1)$ molecules in the condensed phase. Once the “hot” CH_3COCl molecules are formed in the ground electronic state, the α -elimination of HCl can take place easily along the S_0 pathway. Therefore, the internal conversion from the S_1 state followed by the α -elimination in the ground state is the most probable mechanism for formation of HCl in the argon matrix at 11 K.

Mechanistic Aspects

Photoexcitation at 236 nm leads to the gaseous CH_3COCl molecules in the S_1 state. From this state, the CH_3COCl molecules can deactivate via three nonradiative channels: internal conversion (IC) to the ground state, intersystem crossing (ISC) to the T_1 state, and the direct dissociation along the S_1 pathways. The S_1 α -C–Cl bond cleavage occurs in a period of picosecond, IC to the ground state and ISC to the T_1 state are not in competition with the C–Cl direct dissociation along the S_1 pathway. In addition, the α -C–C bond fission has a barrier of 41.4 kcal/mol (139.8 kcal/mol above the S_0 vibrational zero level) on the S_1 pathway. Therefore, the S_1 fission of the α -C–C bond is energetically inaccessible upon photoexcitation at 236 nm (121.1 kcal/mol). The HCl elimination involves breakage and formation of a few bonds simultaneously, the α -elimination of HCl on the S_1 surface takes place with little probability. The present calculations clearly show that the S_1 α -C–Cl bond cleavage is an exclusive channel upon photoexcitation of gaseous CH_3COCl at 236 nm. The C–Cl bond fission was experimentally observed to be the dominant channel in the gas phase.^{4–7} The CH_3CO radicals formed in the α -C–Cl bond cleavage have sufficient internal energy to overcome the barrier on the pathway to $\text{CH}_3 + \text{CO}$. This is consistent with the experimental observation that the four products of Cl, CH_3CO , CH_3 , and CO were found in photolysis of gaseous CH_3COCl by using the FTIR experimental technique.^{8,9} The direct S_1 fission of the α -C–Cl bond is blocked by the matrix effects and the interaction with the matrix results in deactivation of the excited CH_3COCl molecules. As a result, the internal conversion to the ground state becomes the dominant process in the condensed phase, which is followed by the α -elimination of HCl in the ground state.

Acknowledgment. This work was supported by grants from the National Natural Science Foundation of China (Grant Nos. 20472011 and 20233020) and from the Major State Basic Research Development Programs (Grant Nos. 2004CB719903 and 2002CB613406).

Supporting Information Available: Structures and energies for all stationary points reported in the present work, as well as the complete refs 30 and 31. These materials are available free of charge via the Internet at <http://pubs.acs.org>.

References and Notes

- Li, H.; Li, Q.; Mao, W.; Zhu, Q.; Kong, F. *J. Chem. Phys.* **1997**, *106*, 5943.
- Kogure, N.; Ono, T.; Watari, F. *J. Mol. Struct.* **1993**, *296*, 1.
- Shibata, T.; Suzuki, T. *Chem. Phys. Lett.* **1996**, *262*, 115.
- Deshmukh, S.; Hess, W. P. *J. Chem. Phys.* **1994**, *100*, 6429.
- Deshmukh, S.; Hess, W. P. *J. Phys. Chem.* **1994**, *98*, 12535.
- Person, M. D.; Kash, P. W.; Butler, L. J. *J. Chem. Phys.* **1992**, *97*, 355.
- Person, M. D.; Kash, P. W.; Butler, L. J. *J. Phys. Chem.* **1992**, *96*, 2021.
- Rowland, B.; Hess, W. P. *J. Phys. Chem. A* **1997**, *101*, 8049.
- Rowland, B.; Hess, W. P. *Chem. Phys. Lett.* **1996**, *263*, 574.
- Seinfeld, J. H.; Pandis, S. N. *Atmospheric Chemistry and Physics: From Air Pollution to Climate Change*; John Wiley & Sons: New York, 1998.
- Vaida, V.; Solomon, S.; Richard, E. C.; Ruhl, E.; Jefferson, A. *Nature* **1989**, *342*, 405.
- Solomon, S. *Rev. Geophys.* **1988**, *26*, 131.
- Mereau, R.; Rayez, M.-T.; Rayez, J.-C.; Caralp, F.; Lesclaux, R. *Phys. Chem. Chem. Phys.* **2001**, *3*, 4712.
- Li, R.-H.; Wu, J.-C.; Chang, J.-L.; Chen, Y.-T. *Chem. Phys.* **2001**, *274*, 275.
- North, S. W.; Blank, D. A.; Gezelter, J. D.; Longfellow, C. A.; Lee, Y. T. *J. Chem. Phys.* **1995**, *102*, 4447.
- Shibata, T.; Suzuki, T. *Chem. Phys. Lett.* **1996**, *262*, 115.
- N. Kogure, N.; Ono, T.; Suzuki, E.; Watari, F. *J. Mol. Struct.* **1993**, *296*, 1–4.
- Vedova, C. O. D.; Rubio, R. E. *J. Mol. Struct.* **1994**, *321*, 279.
- Tamezane, T.; Tanaka, N.; Nishikiori, H.; Fujii, T. *Chem. Phys. Lett.* **2006**, *424*, 434.
- Francisco, J. S.; Abersold, N. *J. Chem. Phys. Lett.* **1991**, *187*, 354.
- Nimlos, M. R.; Soderquist, J. A.; Ellison, G. B. *J. Am. Chem. Soc.* **1989**, *111*, 7675.
- Sumathi, R.; Chandra, A. K. *J. Chem. Phys.* **1993**, *99*, 6531.
- Winter, P. R.; Rowland, B.; Hess, W. P.; Radziszewski, J. F.; Nimlos, M. R.; Ellison, G. B. *J. Phys. Chem. A* **1998**, *102*, 3238.
- Kudich, A. V.; Bataev, V. A.; Godunov, L. A. *Russ. Chem. Bull.* **2005**, *54*, 62–70.
- Becke, A. D. *J. Chem. Phys.* **1993**, *98*, 1372; Becke, A. D. *J. Chem. Phys.* **1993**, *98*, 5648.
- Lee, C.; Yang, W.; Parr, R. G. *Phys. Rev. B* **1988**, *37*, 785.
- Schmidt, M. W.; Gordon, M. S. *Annu. Rev. Phys. Chem.* **1998**, *49*, 233.
- Frisch, M. J.; Ragazos, I. N.; Robb, M. A.; Schlegel, H. B. *Chem. Phys. Lett.* **1992**, *189*, 524; Yamamoto, N.; Vreven, T.; Robb, M. A.; Frisch, M. J.; Schlegel, H. B. *Chem. Phys. Lett.* **1996**, *250*, 373.
- Dunning, T. H., Jr. *J. Chem. Phys.* **1989**, *90*, 1007; Woon, D. E.; Dunning, T. H., Jr. *J. Chem. Phys.* **1993**, *98*, 1358; Peterson, K. A.; Woon, D. E.; Dunning, T. H., Jr. *J. Chem. Phys.* **1994**, *100*, 7410.
- Frisch, M. J. *et al.* Gaussian 98, Gaussian, Inc.: Pittsburgh, PA 1998.
- MOLPRO is a package of ab initio programs written by Werner, H.-J., et al.
- Cossi, M.; Barone, V.; Robb, M. A. *J. Chem. Phys.* **1999**, *111*, 5295.
- Thompson, D. L., In *Encyclopedia of Computational Chemistry*; Schleyer, P. v. R., Allinger, N. L., Kollman, P. A., Clark, T.; Schaefer, H. F., III, Gasteiger, J., Schreiner, P. R., Eds.; Wiley: Chichester, U.K., 1998; p 3506.
- Bolton, K.; Hase, W. L.; Peshlherbe, G. H.; In *Modern Methods for Multidimensional Dynamics Computation in Chemistry*; Thompson, D. L., Ed.; World Scientific: Singapore, 1998; p 143.
- Helgaker, T.; Uggerud, E.; Jensen, H. J. A. *Chem. Phys. Lett.* **1990**, *173*, 145.
- Millam, J. M.; Bakken, V.; Chen, W.; Hase, W. L.; Schlegel, H. B. *J. Chem. Phys.* **1999**, *111*, 3800.
- Sinnott, K. M. *J. Chem. Phys.* **1961**, *34*, 851.

- (38) Tsuchiya, S.; Iijima, T. *J. Mol. Struct.* **1972**, *13*, 327.
- (39) Durig, J. R.; Davis, J. F.; Guirdis, G. A. *J. Raman Spectrosc.* **1994**, *25*, 189.
- (40) King, R. A.; Allen, W. D. III; Schaefer, H. F. *J. Chem. Phys.* **2000**, *112*, 5585.
- (41) Diau, E. W.-G.; Kotting, C.; Zewail, A. H. *ChemPhysChem* **2001**, *2*, 273.
- (42) Fang, W-H.; Liu, R-Z. *J. Chem. Phys.* **2001**, *115*, 10431.
- (43) Chen, X-B.; Fang, W-H. *J. Am. Chem. Soc.* **2003**, *125*, 9689.
- (44) Sun, L.; Song, K.; Hase, W. L. *Science* **2002**, *296*, 875.
- (45) Ammal, S. C.; Yamataka, H.; Aida, A.; Dupuis, M. *Science* **2003**, *299*, 1555.
- (46) Barltrop, J. A.; Coyle, J. D.; In *Excited States in Organic Chemistry*; Wiley: New York, 1975; p 180.
- (47) Eyring, H.; Lin, S. H.; Lin, S. M. *Basic Chemical Kinetics*; Wiley: New York, 1980.
- (48) Miller, W. H. *J. Am. Chem. Soc.* **1979**, *101*, 220.